

# Tm-doped ZnO: an efficient catalyst for photodegradation of methylene blue under sunlight irradiation

Shirsat Ramesh Natha<sup>1,3,\*</sup>, Manohar Ganpat Chaskar<sup>2</sup>, Yogeshwar Digambar Kaldante<sup>1,3</sup>,  
Yogesh B. Khollam<sup>4</sup>

<sup>1</sup>Department of Chemistry, Baburaoji Gholap College, Sangvi, Pune 411027, Maharashtra, India.

<sup>2</sup>Department of Chemistry, Prof. Ramkrishna More College, Akurdi, Pune 411044, Maharashtra, India.

<sup>3</sup>Department of Chemistry, Annasaheb Waghire College, Otur, Pune 412409, Maharashtra, India.

<sup>4</sup>Department of Physics, Baburaoji Gholap College, Sangvi, Pune 411027, Maharashtra, India.

## Abstract

The pure and Tm-doped ZnO were prepared by environmental friendly approach, involving thermal decomposition of zinc oxalate (ZO) and zinc-thulium oxalate (ZTO) powder respectively obtained by simple mechanochemical method. The process of conversion of ZTO to Tm-doped ZnO was studied with TG-DTG and FTIR spectroscopy. ZnO and Tm-doped ZnO crystallites were characterized by X-ray diffraction (XRD), Field emission scanning electron microscopy (FESEM), Energy dispersive X-ray (EDX) spectroscopy, UV-Visible spectroscopy. The wurtzite crystallite structures of ZnO and Tm-doped ZnO were revealed from X-ray diffraction data. The peak broadening and higher Bragg angle shift in XRD pattern of Tm-doped ZnO as compared to the pure ZnO confirmed the insertion of Tm into ZnO lattice. The morphological study using FESEM confirmed nanocrystalline nature of ZnO and Tm-doped ZnO with nearly uniform particles size distribution. EDX study confirmed the purity of ZnO and Tm-doped ZnO. The chemical bonding information was obtained from FTIR spectra and band gap was determined from UV-Visible spectroscopy. Photocatalytic activity of ZnO and Tm-doped ZnO was tested by means of photocatalytic degradation of methylene blue under irradiation of sunlight in a batch photoreactor. The complete photocatalytic degradation of 50 ppm methylene blue is achieved over 150 mg /100 ml loading of Tm-doped ZnO at pH 9 within 6 h irradiation of sunlight. The degradation efficiency of Tm-doped ZnO is found to be greater than that of pure ZnO.

**Keywords:** ZnO; Tm-doped ZnO; Zinc thulium oxalate; Photodegradation; Methyl orange.

## 1. Introduction

Present scenario of rapidly changing technological world seeking the need of nano system for economy [1]. For such perspectives, we are observing the revolutionary changes for synthesis of nano sized materials. The aims and objectives for syntheses are directed towards more reactive, easily available, cheap and sustainable materials in field of science and technology viz. spintronics, optoelectronics, quantum computing and photocatalysis [2]. In present situation, the

energy sources and clean water for survival is becoming an urgent need for mankind [3]. Solution can be given from different sources as needs are different. Easier way for finding solution is only photocatalysis. Splitting of water to produce clean hydrogen fuel and degradation of pollutant in fresh water are possible by applying photocatalysis. So photocatalysis only a single way for achieving both the tasks [4]. As it is commonly known, photocatalysis is driven only in presence of a semiconducting oxides and UV/visible light. With this knowledge, attempts are being devoted and explored for achieving the economy and efficiency in photocatalysis. Various pure metal oxides such as ZnO, TiO<sub>2</sub>, WO<sub>3</sub> etc. are regularly utilized for photocatalysis [5]. As water is major source for hydrogen generation under photocatalytic splitting, choice of photocatalysts can be selective and limited [6]. But for degradation of variety of dyes and pollutants, the list of photocatalysts is required to be numerous with selectivity for given substrates [7]. In searching of different pure photocatalysts for given dye is very laborious. To circumvent this tedious job, it is very important to modify the reactivity and selectivity in given pure metal oxides. ZnO is very popular semiconductor opted for most of the photocatalytic dye degradation [8]. Although various newer methods introduced for ZnO for dye degradation, economy and selectively can be achieved by modification of electronic and surface structure. The applicability of photocatalytic degradation is limited by absorption of light in visible region and rate of recombination of electron hole pairs [9]. For efficient and economic photocatalysis, the absorption of visible light for generation of electron-hole pairs and separation of electron-hole pairs is very important. Both targets can be achieved by introducing extrinsic defects in ZnO [10]. It is observed that, extrinsic defects in ZnO can be created by doping rare earth metal ions in crystal structure of ZnO [11]. Erbium doped ZnO nanocrystals synthesized by sol gel method [12], Europium doped ZnO was synthesized by hydrothermal method [13] Yb doped ZnO synthesized by wet chemical method [14], Sm-doped ZnO using CVD technique [15].

In present study we are summarizing the environmental friendly synthesis of pure ZnO and Tm-doped ZnO involving thermal decomposition of zinc oxalate (ZO) and zinc thulium oxalate (ZTO) powders respectively obtained by simple mechanochemical method. The Tm-doped ZnO synthesized by this method shows better solar photocatalytic degradation efficiency for methylene blue than that of pure ZnO. Parameters such as amount of photocatalyst, concentration of dye, pH, etc. on photocatalytic degradation of methylene blue are studied.

## 2. Experimental

### 2.1. Materials

In present study, zinc acetate, oxalic acid, thulium acetate and methylene blue of analytical grade obtained from S.D. Fine Chemicals Pune, India were used as starting materials without further any purification. The appropriate concentration of methyl orange solutions was prepared

by using double distilled water. The pH of the solutions were adjusted to desired values from 5 to 10 with H<sub>2</sub>SO<sub>4</sub> (0.01 N) and NaOH (0.01 N).

## 2.2. Synthesis of photocatalyst powders

Thulium-doped zinc oxide was prepared by two-step process. It involves solution free mechanochemical synthesis of zinc thulium oxalate (ZTO) powders followed by thermal decomposition of ZTO to form Tm-doped ZnO. In this synthesis, mixture of 0.95 M of zinc acetate dihydrate and 1.1 M of oxalic acid was mixed thoroughly for 10 min. at room temperature to obtain zinc oxalate dihydrate. Then 0.05 M of thulium acetate was added to this mixture with continuous grinding and after 20 min. zinc thulium oxalate (ZTO) was obtained. The calcination of ZTO at 400 °C was resulted into the formation of Tm-doped ZnO. Without adding thulium acetate, the same procedure was repeated to obtain zinc oxalate (ZO) and pure ZnO for comparison [16] purpose.

## 2.3. Equipments

The temperature conversion of ZTO to Tm-doped ZnO was obtained by thermal gravimetric analysis machine (Shimadzu, TG - DTG - 60H) and FTIR (Shimadzu, FTIR-Miracle 10) spectrometer equipped with KBr beam splitter). The X-ray diffraction (XRD) patterns of the Tm - doped ZnO powder was obtained by using X-ray Diffractometer (Miniflex-600, CuK<sub>α</sub> radiation, λ = 1.5406 Å). The mean crystallite size (D) of the particles was determined from the XRD line-broadening measurement from the Debye-Scherer equation [17] as follows:

$$D = \frac{0.89\lambda}{(\beta \cos\theta)} \quad (1)$$

Where, λ = wavelength (CuK<sub>α</sub>), β = full width at the half maximum of (101) peak and θ = diffraction angle. The morphological analysis of powder was done by using FESEM (JEOL JSM-6360A). The elemental characterization of the powder was studied with energy dispersive X-ray spectra (EDX). The photocatalytic reactions were carried out at ambient temperature under the irradiation of sunlight in batch photo-reactor. The initial pH of suspension was recorded with the help of pH meter (Equiptronics). The extent of photocatalytic degradation (PCD) at an interval of 1 h under sunlight irradiation was primarily checked by means of decrease in absorbance of the dye solution measured using UV-visible spectrophotometer (Systronics), intensity of sunlight was periodically checked by LUX meter.

## 2.4. Photocatalytic degradation experiments

All photocatalytic reactions were carried out in batch photo-reactor configured with cylindrical glass vessel (250 ml capacity), quartz cool trap and magnetic stirrer. A known quantity (50, 100, 150, 200, 250 and 300 mg) of Tm-doped ZnO was added in methyl orange solution in water. This mixture was agitated in an ultrasonic bath for 5 min. to obtain uniform suspension. Initial pH of suspension was recorded. Whole setup was then placed in sunlight with constant stirring for specific period of time between 10:00 a.m. and 4:00 p.m. The extent of degradation at an interval of 1 h under sunlight irradiation was primarily monitored with spectrophotometric absorbance measurement and the percent degradation was calculated from the following expression:

$$\% D = \left[ \frac{A_0 - A_t}{A_0} \right] \times 100 \quad (2)$$

Where, % D - percent degradation,  $A_0$  - initial absorbance,  $A_t$  - absorbance at time t. The average photon flux calculated from periodic measurement of sunlight intensity for entire duration of irradiation was found to be  $1.68 \times 10^{-7}$  Einstein  $s^{-1} cm^{-2}$ .

## 3. Result and discussion

### 3.1. Thermal gravimetric analysis

Fig. 1 shows the TG-DTG plots for ZTO powder. The thermal decomposition of ZTO occurred with endothermic and exothermic effects. There are three major weight losses from 40 °C to 400 °C in TG curve. The 2.98 % weight loss from 30 °C to 120 °C is assigned to the loss of residual acetic acid. The 18.70 % weight loss from 76 °C to 227 °C is due to adsorbed water and removal of remaining acetic acid by-product. The acetic acid molecules easily volatilized into atmosphere during the process of grinding. However, due to partial non volatility (boiling point 118 °C), rest of the acetic acid can only be totally removed at a temperature above 118 °C. The dehydration and removal of acetic acid at 120 °C to 147 °C from ZTO accomplished with endothermic effect as reflected in DTG. The 36.63 % weight loss from 227 °C to 400 °C in TG curve is attributed to decomposition of oxalate moiety of ZTO to form Tm-doped ZnO. This is seen in terms of broad exothermic peak in DTG centered at 400 °C. The DTG curve shows three major peaks centered at 74.5 °C, 147 °C and 388 °C corresponding to the weight losses in TG curve. From this, it is clear that temperature for the conversion of ZTO into Tm-doped ZnO is 400 °C.

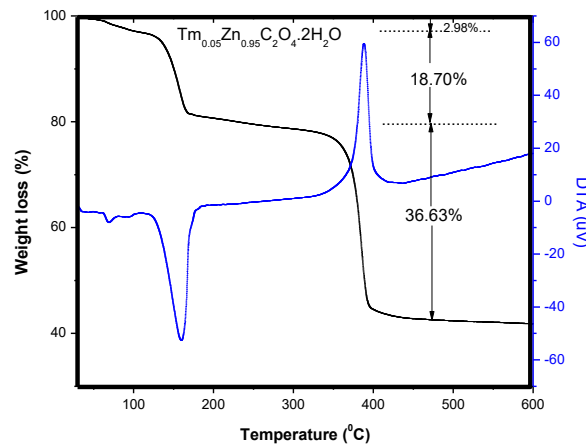


Fig. 1 TG-DTG plots for ZTO precursor powder

### 3.2. FTIR analysis

The FTIR spectra of ZTO and Tm-doped ZnO are shown in fig. 2. The Tm-doped ZnO was obtained by thermal decomposition of ZTO precursor. Fig. 2 shows the changes FTIR spectra during thermal decomposition of ZTO to Tm-doped ZnO. In FTIR spectrum of ZTO, the band at  $3385\text{ cm}^{-1}$  is due to the stretching vibration of O-H in water of crystallization. The band at  $1635\text{ cm}^{-1}$  is due to C=O stretching vibration. The bands at  $1360\text{ cm}^{-1}$  and  $1315\text{ cm}^{-1}$  are due to C-O stretching vibration and the band at  $418\text{ cm}^{-1}$  is due to Zn-O bonding. When ZTO is heated at  $400\text{ }^{\circ}\text{C}$  all bands except at  $418\text{ cm}^{-1}$  are found to be disappeared. This FTIR spectra results support the TG-DTG analysis.

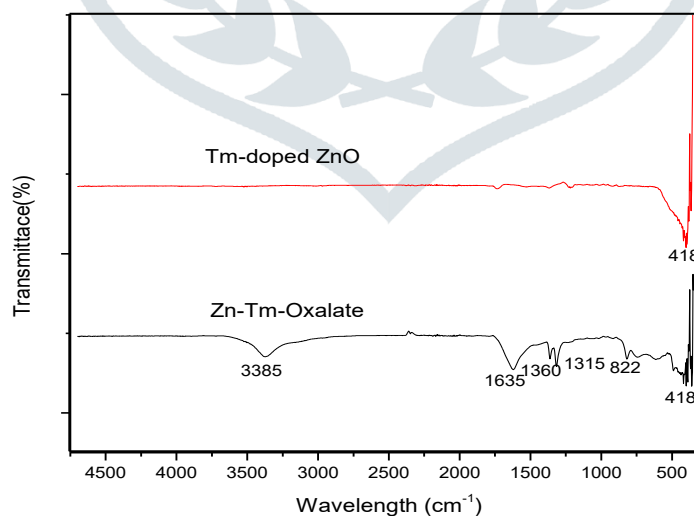


Fig. 2: FTIR spectra for ZTO and Tm-doped ZnO powders

### 3.3. XRD Analysis

Fig. 3 (left) shows the XRD patterns of ZnO and Tm-doped ZnO powders. From this XRD patterns, peaks are observed at  $2\theta = 31.70^\circ, 34.36^\circ, 36.20^\circ, 47.52^\circ$  and  $56.58^\circ, 62.82^\circ, 66.38^\circ, 67.92^\circ, 69.06^\circ, 72.52^\circ, 76.88^\circ$  for ZnO powder and at  $2\theta = 31.88^\circ, 34.54^\circ, 36.38^\circ, 47.66^\circ, 56.70^\circ, 62.96^\circ, 66.44^\circ, 68.04^\circ, 69.18^\circ, 72.88^\circ, 77.04^\circ$  for Tm-doped ZnO powder. This data is noted to be in good agreement with the data given in JCPDS card number 36-1451 for ZnO. The peaks are indexed to the (100), (002), (101), (102), (110), (103), (200), (112), (201), (004), and (202) planes of wurtzite structure of ZnO. The higher values of  $2\theta$  for different XRD peaks in case of Tm-doped ZnO as compared to the corresponding values of  $2\theta$  in case of pure ZnO is due to substitution of Tm at Zn sites. Fig. 3 (left) shows the slow scans of (101) reflections of corresponding XRD patterns (right) in  $2\theta$  range of  $35.6$  to  $37.0^\circ$ . These slow scans are used to find crystallite size of pure and Tm-doped ZnO by using Debye-Scherrer relation given in equation (1). The crystallite size obtained for ZnO and Tm-doped ZnO are found to be  $37.97$  nm and  $31.14$  nm respectively. Incorporation of Tm in the ZnO lattice produces distortion of structure of some crystallite planes of ZnO. This is reflected in the (i) shifting of Bragg's diffraction peaks towards the higher angle side and (ii) peak broadening in case of Tm-doped ZnO as compared to ZnO [11].

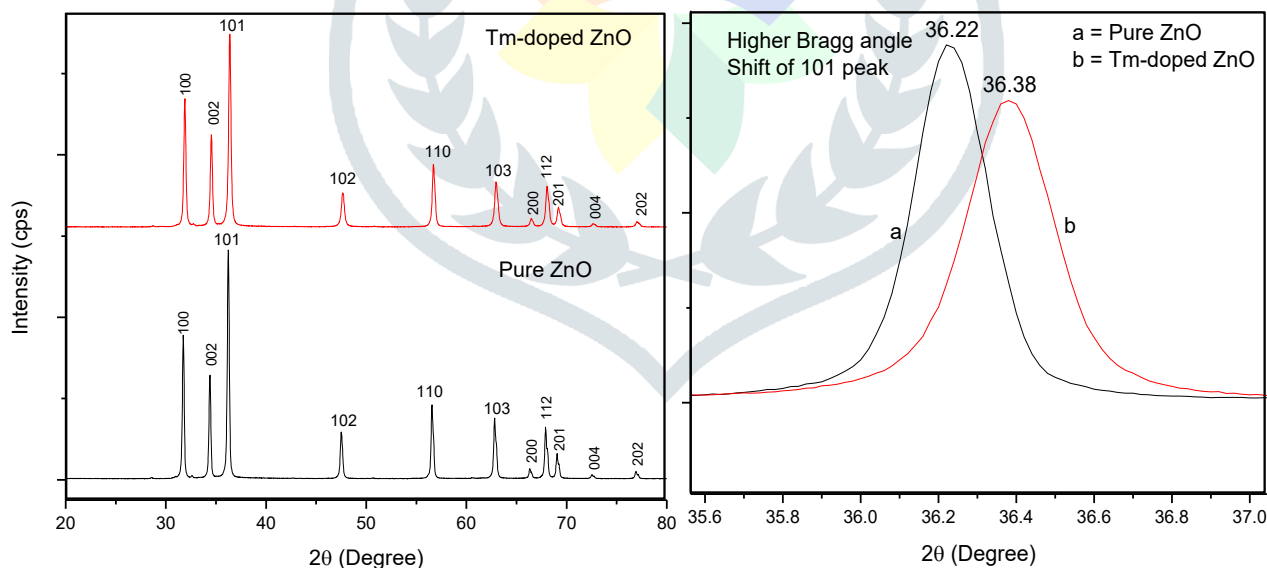


Fig. 3 XRD patterns of Pure ZnO and Tm-doped ZnO powders (left) and slow scans of corresponding XRD patterns (right) in  $2\theta$  range of  $35.6$  to  $37.0^\circ$

### 3.4. FESEM analysis

The morphology of ZnO and Tm-doped ZnO powders was studied by using field emission scanning electron microscopy (FESEM) studies. Fig. 4 shows the FESEM photographs of pure ZnO and Tm-doped ZnO powders. The FESEM photograph of ZnO powder shows the single

homogeneous phase with hexagonal morphology of the particles. The particles are non-agglomerated and hard. The particle size distribution is found to be nearly uniform. The average particle size is found to be around 100 nm. The FESEM photograph of Tm-doped ZnO shows mixed morphology of particles. The hexagonal as well as spherical particles are observed in image. The particles are non-agglomerated and hard. In this case, the particle size distribution is also found to be nearly uniform. The average particle size is found to be around 50 nm. Thus both pure ZnO and Tm doped ZnO powders are nanocrystalline. The reduction in average particle size in case of Tm doped ZnO powder might be due to the incorporation of Tm in ZnO lattice at Zn sites.

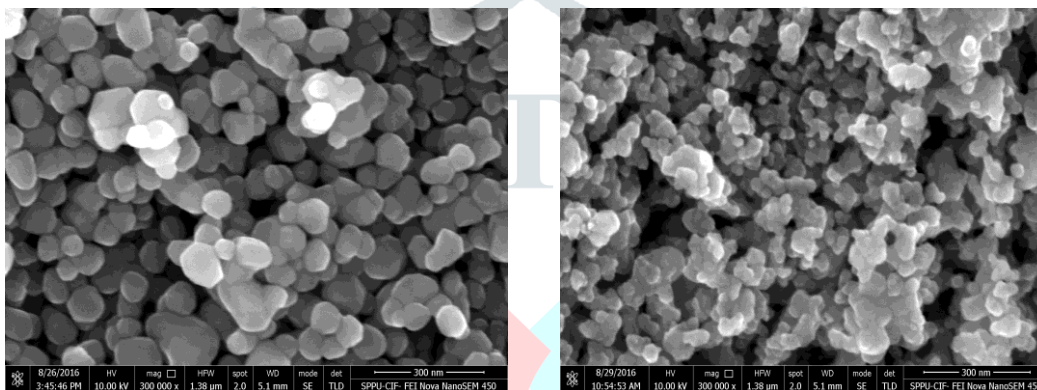


Fig. 4 FESEM photographs of pure ZnO (left) and Tm-doped ZnO (right) powders.

### 3.5. EDX analysis

Fig. 5 shows energy dispersive X-ray (EDX) spectra of pure ZnO and Tm-doped ZnO powders. The EDX spectrum of ZnO powder shows peaks corresponding to Zn and O only and that of EDX spectrum of Tm-doped ZnO powder shows peaks corresponding to Zn, O and Tm only. These spectra clearly indicate purity of the both pure ZnO and Tm-doped ZnO powders. Further, the presence of Tm in case of Tm-doped ZnO powder indirectly might support the incorporation of Tm in ZnO lattice.

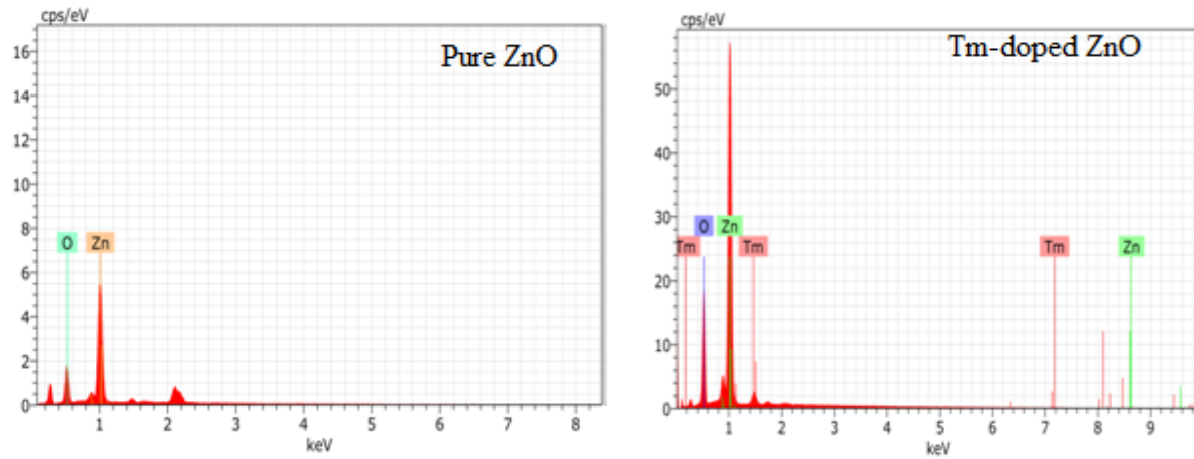


Fig. 5 EDX analysis of Pure ZnO and Tm-doped ZnO powders

### 3.6. UV-visible analysis

Fig. 6 shows UV-visible spectra of pure ZnO and Tm-doped ZnO powders. The UV-visible spectra of ZnO and Tm-doped ZnO powders show distinctly situated extinction bands in the range of 390 nm and 410 nm. It implies that, incorporation of Tm in ZnO lattice shifts the absorption wavelength ( $\lambda_{\max}$ ) 393.8 nm of ZnO towards longer wavelength 408.4 nm. The values of the band gap for ZnO and Tm-doped ZnO powders are obtained from the UV-Visible spectra. The decrease in the band gap energy of ZnO from 3.183 eV to 3.057 eV on Tm-doping, suggest the presence of more number of absorption states in Tm-doped ZnO than pure ZnO.

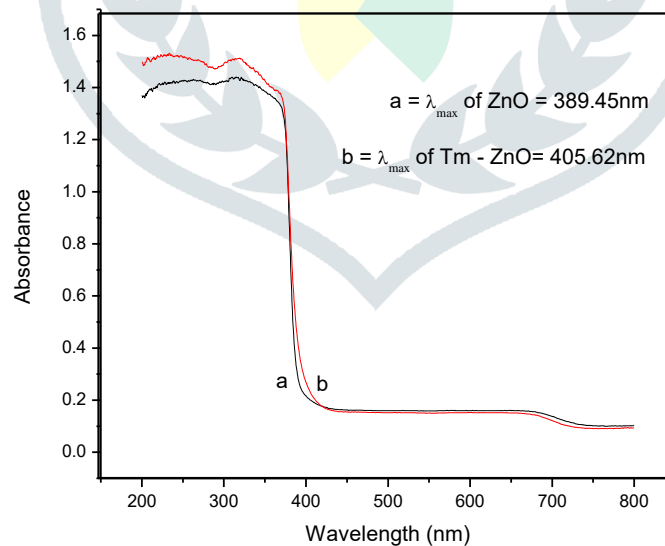


Fig. 6 UV-visible spectra of pure ZnO and Tm-doped ZnO powders

### 3.7. Photocatalytic activity

#### 3.7.1. Effect of initial concentration of substrate

The degradation efficiency of methyl orange over pure ZnO and Tm-doped ZnO at different initial concentrations in the range 25 - 150 ppm was investigated as a function of sunlight irradiation time at the pH 10 of the suspension. The degradation efficiency is measured in terms of decrease in the absorbance (increase in % degradation) of methylene blue and results are illustrated in Fig. 7. The 50 ppm methylene blue was mineralized by using 150 mg/100 mL of Tm-doped ZnO powder. It shows increase in degradation efficiency than that of pure ZnO. However, after 50 ppm, degradation efficiency was found to be inversely affected by concentration of methylene blue. With increase in the concentration of methylene blue the dye solution becomes more intense colored and hence light photons cannot reach the surface of photocatalyst easily. This results in decreased absorption of photons by the photocatalyst and consequently the degradation efficiency was reduced. This shows that, Tm-doped ZnO is effective photocatalyst than ZnO under solar light irradiation. From this study 50 ppm optimum concentration of methylene blue was selected for the study of other parameters.

#### 3.7.2. Effect of amount of photocatalyst

Fig. 8 shows degradation of 50 ppm methylene blue containing 50 to 300 mg/100 ml quantities of photocatalyst loading in sunlight irradiation. The degradation efficiency was gradually increased up to 150 mg /100 mL and then it was decreased. At lower photocatalyst loading level than the optimum amount, photonic absorption controls the degradation efficiency due to limited surface area of photocatalyst. The number of active sites on the photocatalyst surface and hence the number of hydroxyl, and superoxide radicals increases with increase in the amount of photocatalyst. The photocatalyst loading above optimum level results in decrease of degradation efficiency results from the shadowing effect due to more turbid solution formation, which prevents the penetration depth of solar radiation. Hence, the optimal photocatalyst loading of 150 mg/100 mL was selected throughout the present study.

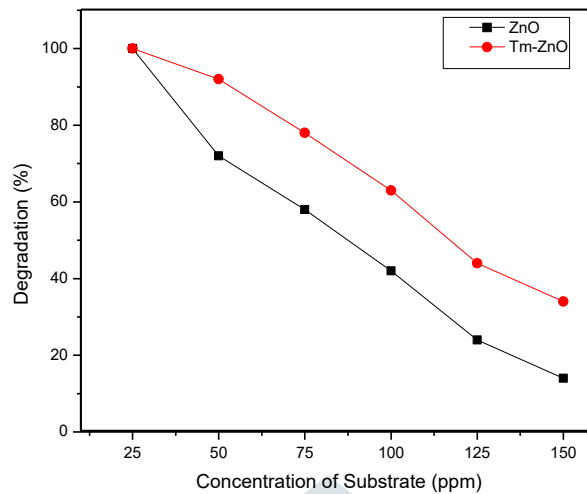


Fig. 7 Variation of percentage degradation with concentration of substrate (ppm) for pure ZnO and Tm-doped ZnO powders

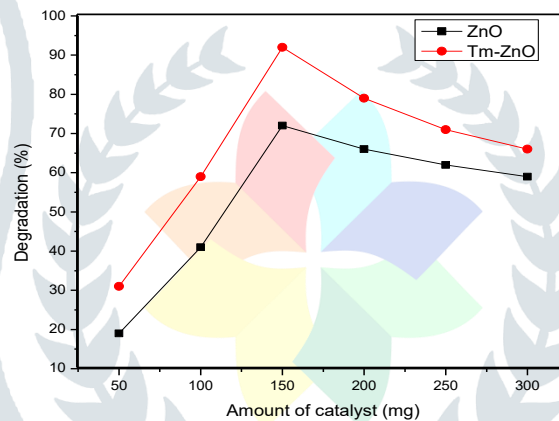


Fig. 8 Variation of percentage degradation with amount of catalyst for pure ZnO and Tm-doped ZnO powders

### 3.7.3. Effect of pH of suspension

The effect of initial pH of suspension on degradation efficiency was studied from 5 to 12 with 50 ppm methylene blue solution and 150 mg /100 mL photocatalyst loading. The pH of the suspension was adjusted only before irradiation with sunlight and it was not controlled during the course of reaction. All other parameters were kept constant. In agreement with well-known fact pure ZnO shows lower degradation efficiency in acidic medium due to slight (< 1 %) dissolution. The extent of methylene blue degradation was found to increase with increase in initial pH of suspension (Fig. 9). In alkaline medium, excess of hydroxyl anions promotes photogeneration of hydroxyl radicals, which are primary oxidizing species in the photodegradation. The degradation efficiency of ZnO and Tm-doped ZnO was declined for higher pH (10 - 12) of the suspension

due to the formation of more turbid solution. Hence, the optimal pH of suspension was found to be 9 for the photocatalytic degradation of methylene blue with pure ZnO and Tm-doped ZnO.

### 3.7.4. Effect of irradiation time

The degradation efficiency of ZnO and Tm-doped ZnO in sunlight gradually increases with increase in irradiation time (fig. 10). The 50 ppm methylene blue solution was completely mineralized over 150 mg/100 ml Tm-doped ZnO at the pH 9. It is observed that with increase in irradiation time, the absorbance of methylene blue was found to decrease and it becomes nearly zero after 6 h irradiation of sunlight (fig. 11). Thus 6 h irradiation time is optimum for the degradation of methylene blue as well as ZnO and Tm-doped ZnO proven to be an effective photocatalysts in sunlight.

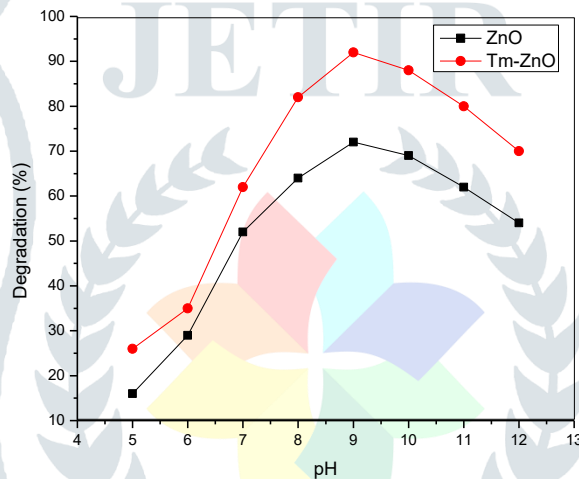


Fig. 9 Variation of percentage degradation with pH of suspension for pure ZnO and Tm-doped ZnO powders

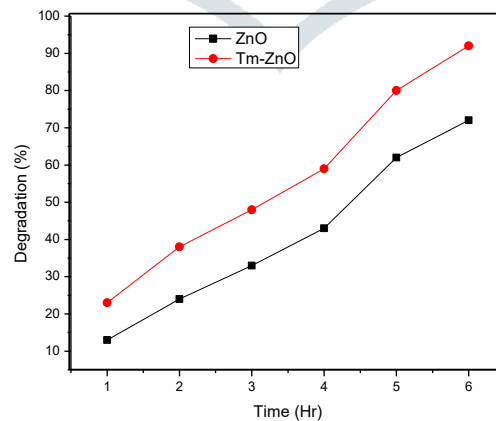


Fig. 10 Effect of irradiation time on percent degradation efficiency

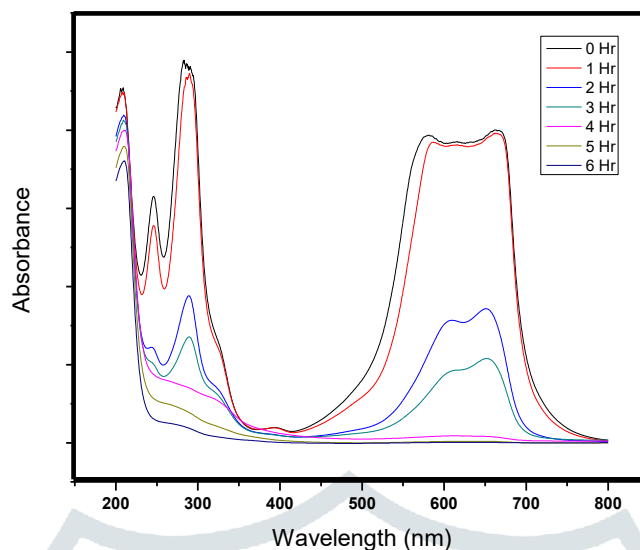


Fig. 11 UV-Visible spectra showing photocatalytic degradation

#### 4. Conclusions

In present study, pure and Tm-doped ZnO are synthesized by solvent free and environment friendly mechanochemical method. The ZO and ZTO powders calcined at 400 °C resulted in ZnO and Tm-doped ZnO particles respectively, as confirmed by UV-Visible spectroscopy, FTIR spectroscopy, XRD, FESEM and EDX studies. The peak broadening and higher Bragg angle shift (by  $0.16^\circ$ ) in XRD pattern of Tm-doped ZnO as compared to the pure ZnO confirmed the insertion of Tm into ZnO lattice. The complete photocatalytic degradation of 50 ppm methylene blue is achieved over 150 mg /100 ml loading of Tm-doped ZnO at pH 9 within 6 h irradiation of sunlight. The degradation efficiency of Tm-doped ZnO is found to be greater than that of pure ZnO.

#### References

- [1] V. Sharma, U. Sharma, M. Chattopadhyay, V. N. Shukla, *Materials Today: Proceedings*, 5 (2018) 6376 - 6380.
- [2] A. Kołodziejczak - Radzimska, T. Jesionowski, *Materials*, 7 (2014) 2833 - 2881.
- [3] Prashant V. Kamat, Juan Bisquert, *J. Phys. Chem. C*, 117 (2013) 14873 - 14875.
- [4] J. Lijuan, W. Yajun, F Changgen, *Procedia Engineering*, 45 (2012) 993 - 997.
- [5] J. Xing, W. Qi Fang, H. Zhao, H. G. Yang, *Chem. Asian J.*, 7 (2012) 642 - 657.
- [6] C. A. Grimes, O. K. Varghese, S. Ranjan, (2008) *Hydrogen Generation by Water Splitting*. (eds) Light, Water, Hydrogen. Springer, Boston, MA.
- [7] A. Kumar, G. Pandey, *Mater. Sci. & Engg. Inter. J.*, 1 (2017) 1 - 10.

- [8] K. Intarasuwan, P. Amornpitoksuka, S. Suwanboon, P. Graidist, Separation and Purification Tech., 177 (2017) 304 - 312.
- [9] A. B. Lavand, Y. S. Malghe, J. King Saud University – Science, 30 (2018) 65 - 74.
- [10] T. L. Tan, C. W. Lai, S. B. Abd Hamid, J. Nanomaterials, (2014) 1 - 6.
- [11] D. Daksh, Y. K. Agrawal, Reviews in Nanoscience and Nanotechnology, 5 (2016) 1 - 27.
- [12] R. Vettumperumal, S. Kalyanaraman, R. Thangavel, J. Luminescence 158, (2015) 493.
- [13] M. Najafi, H. Haratizadeh, Solid State Sci., 41 (2015) 48.
- [14] N. Jiang, S. Ye, B. Yang, Mater. Chem. Phys., 142 (2013) 37.
- [15] T. Tsuji, Y. Terai, M. H. B. Kamarudin, M. Kawabata, Y. Fujiwara, J. Non-Crystalline Solids, 358 (2012) 2443.
- [16] S. K. Pardeshi, A. B. Patil, J. Mol. Catal. Chem., 308 (2009) 32 - 40.
- [17] L. Wu, J. -C. Yu, X. Fu, J. mol. Catal. A: Chem., 244 (2006) 25 - 32.

